THERMAL BEHAVIOR OF AIR-FLUID IN TRIANGULAR CAVITIES OF 3D PRINTED CONCRETE WALLS

Rodrigo do Val Andrade[1], Henrique Conde Carvalho de Andrade[1], Oscar Aurelio Mendoza Reales[1], Ana Beatriz de Carvalho Gonzaga e Silva[1,2], Eduardo de Moraes Rego Fairbairn[1]

[1] *Civil Engineering Program -COPPE, Federal University of Rio de Janeiro*
Cidade Universitária, Zip-Code 21945-970, Rio de Janeiro/RJ, Brazil.
rodrigo.andrade@coc.ufrj.br, oscar@coc.ufrj.br, anabeatrizgonzaga@coc.ufrj.br, eduardo@coc.ufrj.br, henriqueconde@coc.ufrj.br
[2]*Department of Structures – Polytechnic School, Federal University of Rio de Janeiro*
Cidade Universitária, Zip-Code 21945-970, Rio de Janeiro/RJ, Brazil

Abstract. The civil construction industry has shown increasing interest in 3D printing technology due to its ability to produce highly complex structures with different internal wall geometries using concrete as the raw material. With the advancement of technology, numerical modeling software has become necessary to simulate heat transfer and the thermal performance of objects developed through 3D printing. This study aims to simulate the thermal behavior of air-fluid within two different triangular cavities in a 3D-printed wall using ANSYS software. The research performed two computational simulations considering gravity and two simulations under zero-gravity conditions. These simulations aim to analyze fluid velocity, temperature distribution, and temperature profile within the cavities, highlighting the influence of gravity on heat transfer and thermal behavior.

Keywords: 3D printed concrete, Computational Modeling, Thermal Behavior.

1 Introduction

Industry 4.0, with 3D printing as one of its main innovations, is revolutionizing various fields, including construction. Concrete 3D printing technology has rapidly developed in recent years, standing out for its efficiency and feasibility in large-scale automated construction [1], promoting significant changes in the construction industry by creating solid objects through layer-by-layer material deposition. The growing interest in the sector has resulted in studies on the efficiency of 3D-printed technology compared to conventional methods [2].

In addition to advantages such as cost and construction time reduction, a less researched aspect is the thermal behavior of structures involving 3D-printed concrete. In conventional buildings, heat transfer by thermal convection occurs in the air cavities of the masonry. Due to the temperature difference between its layers, air currents are generated, which, due to the low thermal conductivity of the air, reduce heat transfer from the outside to the inside of the building. 3D printing walls have similar thermal phenomena; however, the geometric freedom provided by 3D printing technology allows for the optimization of these characteristics, making it possible to design air cavities with specific shapes that increase thermal efficiency, improve resistance to heat flow, and, consequently, increase the energy efficiency of buildings [3].

In this context, this article analyzes the thermal behavior of air in two triangular cavities of a 3D printed wall prototype, using ANSYS software to perform computational fluid dynamics (CFD) simulations, investigating the air-fluid velocity, temperature distribution, and temperature profile within the cavities, and highlighting the influence of gravity on heat transfer and thermal behavior.

2 Experimental Model

A wall prototype developed by 3D printing in concrete is presented [3] with air cavities in a triangular shape. This setup is designed to analyze the thermal performance of the structure, investigating how internal geometric shapes can influence the thermal behavior of 3D-printed walls since filaments can create preferential paths for heat transfer. The printed wall was subjected to a heating test to evaluate the temperature distribution along the wall. To ensure the accuracy of the results, the thermocouples were positioned on the concrete filaments and in the triangular air cavities, allowing temperature monitoring at different points over time. Figure 1 presents the temperatures recorded by thermocouples 4, 5, 6, and 7 after 5 hours and 30 minutes of heating.

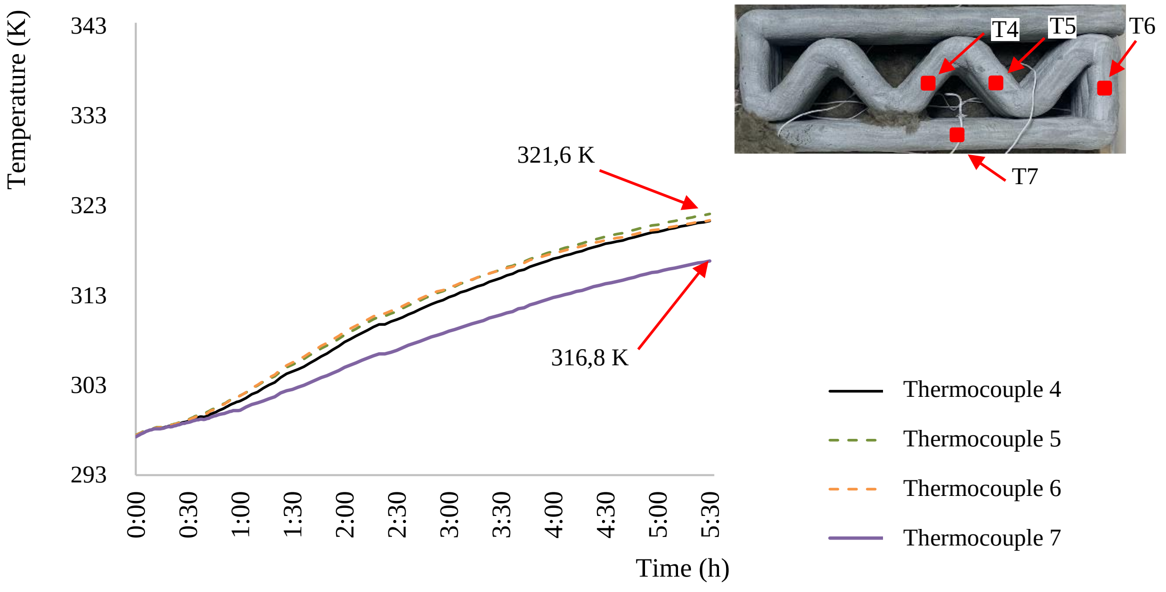

Figure 1. Temperature graph over time for thermocouples 4, 5, 6 and 7 during the experimental test.

Figure 2 depicts the temperature inside the air cavity, used as the initial temperature condition for the simulations.

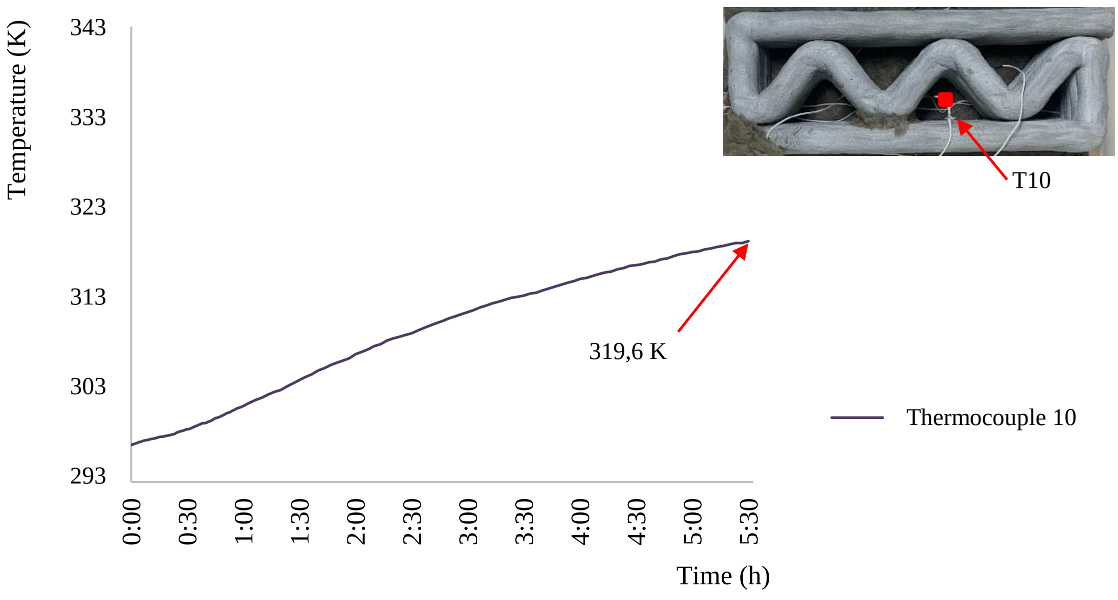

Figure 2. Temperature graph over time for thermocouple 10 during the experimental test.

3 Computational Model

3.1 Definition of the mathematical model

To understand the thermal processes that influence the behavior of the air-fluid within the cavities of the triangular prisms, the mathematical model [4] for fluid in a continuous medium was applied, considering the laws of conservation of mass, momentum, and energy. The law of conservation of mass is presented in equation (1).

$$\frac{\partial \rho}{\partial t} + \nabla \cdot \left(\rho \vec{V}\right) = 0 \tag{1}$$

Where $\vec{V}$ is the velocity vector of the air-fluid, whose components are $\vec{V} = (u_x, u_y, u_z)$. Based on Newton's second law, the Navier-Stokes equations (2 - 4) are used to describe the conservation of momentum in the x, y, and z directions.

$$\frac{\partial(\rho u_x)}{\partial t} + \nabla\left(\rho u_x \vec{V}\right) = -\frac{\partial p}{\partial x} + (\rho - \rho_0) g_x + (F_x)_{viscous} \tag{2}$$

$$\frac{\partial(\rho u_y)}{\partial t} + \nabla\left(\rho u_y \vec{V}\right) = -\frac{\partial p}{\partial y} + (\rho - \rho_0) g_y + \left(F_y\right)_{viscous} \tag{3}$$

$$\frac{\partial(\rho u_z)}{\partial t} + \nabla\left(\rho u_z \vec{V}\right) = -\frac{\partial p}{\partial z} + (\rho - \rho_0) g_z + (F_z)_{viscous} \tag{4}$$

Where F_x, F_y and F_z are the viscous stress of Newtonian fluids, p is the pressure, ρ is the fluid density and g is the gravitational acceleration component, $\vec{V}$ is the velocity vector of the air-fluid and. The energy equation in this scenario can be simplified into the temperature transport equation (5):

$$\frac{\partial(\rho c_p T)}{\partial t} + \nabla \cdot \left(\rho c_p \vec{V}\, T\right) = \nabla \cdot (k \nabla T) \tag{5}$$

Where ρ is the fluid density, c_p is the specific heat capacity at constant pressure, k is the thermal conduction coefficient, $\vec{V}$ is the velocity vector of the air-fluid, and T is the temperature.

3.2 Geometry definition

The geometric characteristics were defined based on the experimental test of a prototype 3D-printed concrete wall conducted by [3]. The experimental wall has six triangular air cavities, two of which have different dimensions. Larger cavities are located closer to the center of the wall, while smaller cavities are located near to the side of the wall. For a three-dimensional analysis of the air-fluid, triangular cavities were used, as shown in Figure 3. The cavities closest to the center of the wall measure 14.80 cm along the X-axis and 6.20 cm along the Z-axis. The cavities closer to the sides measure 7.40 cm along the X-axis and 6.20 cm along the Z-axis. The height of all cavities, corresponding to the Y-axis where gravity acts, is 10 cm.

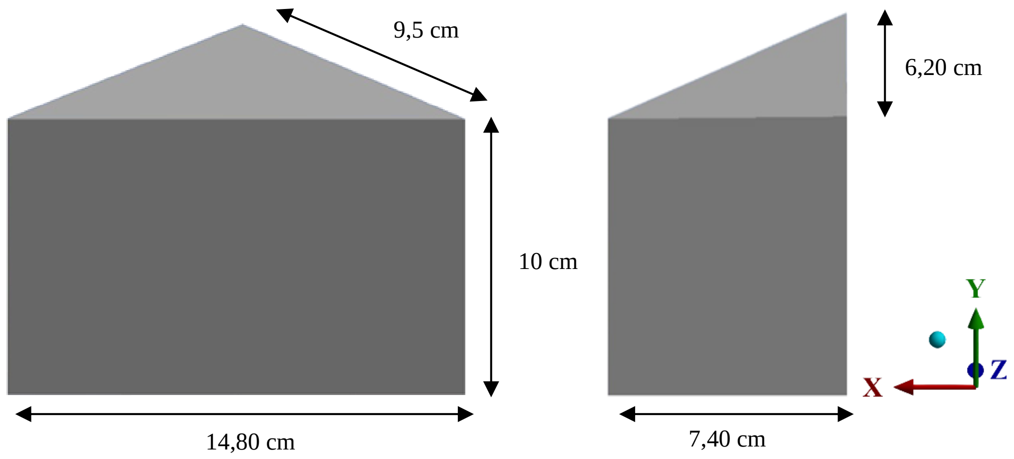

Figure 3. Schematic representation of cavity 1 (left) and cavity 2 (right).

3.3 Mesh

The meshes used in the simulations of the air-fluid in the two cavities are shown in Figure 4. This meshes were generated using ANSYS Fluent software and features a quadratic distribution of elements along the geometry. To optimize results, the mesh was divided into 156,800 and 102,789 elements for cavities 1 and 2, respectively.

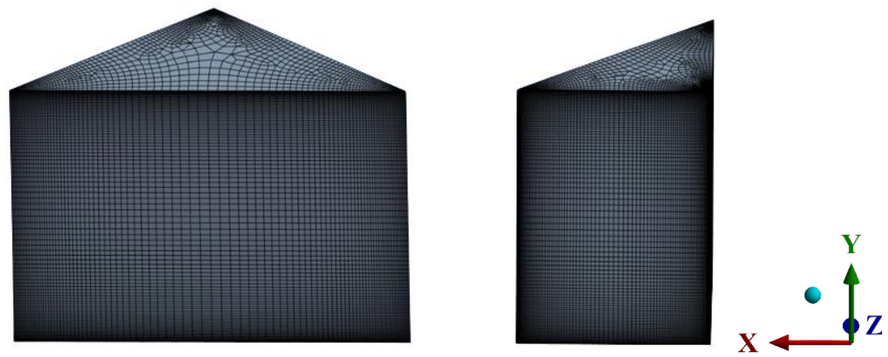

Figure 4. Representation of the meshes used in the air-fluid simulations.

3.4 Initial and boundary conditions

This topic shows the two different triangular prism air cavity configurations, as well as the initial and boundary conditions applied for the thermal analysis. Each geometry contains two triangular and three rectangular faces. The triangular faces are treated as adiabatic, meaning that the heat flow is zero in these regions, which prevents thermal exchange with the external environment. The rectangular faces are configured with the initial temperatures found in the experimental model: the T4, T5, and T6 faces were adjusted to 321.6 K and the T7 face to 316.8 K. The fluid velocity and pressure on all surfaces were set as zero. The simulation parameters include the analysis of the behavior of the fluid inside the cavities for 5 minutes. The conditions applied to the models, identified as cavity 1 (right) and cavity 2 (left), are illustrated in Figure 5.

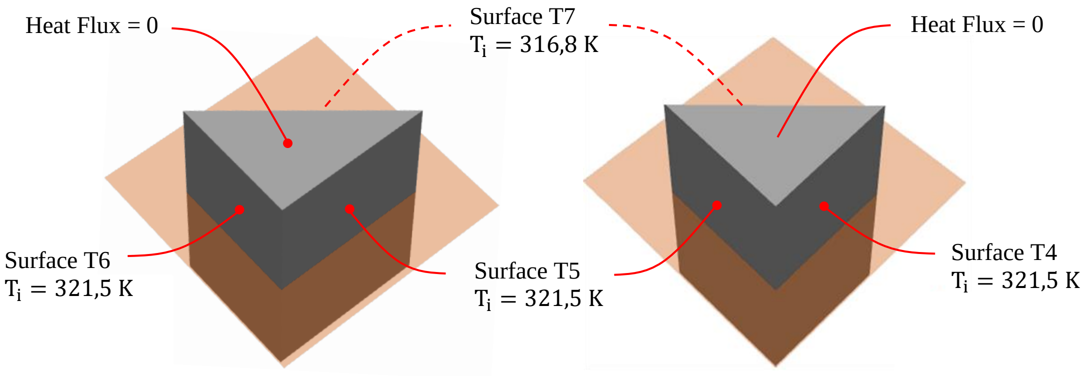

Figure 5. Thermal conditions on the surfaces of cavities 1 (right) and 2 (left), with initial temperatures and zero heat flux

During modeling, the cavities were defined as air-fluid. The density was modeled as an ideal incompressible gas, and the properties of specific thermal capacity (Cp), thermal conductivity, and viscosity were kept constant throughout the simulation process. The specific values of these properties are presented in Table 1.

Table 1. Properties of the air fluid used in the simulations

Thermal Properties:	Value
Specific Heat Capacity (Cp)	1006,43 [J/kgK]
Thermal Conductivity (k)	0,0242 [W/mK]
Viscosity (ν)	1,7894e-05 [kg/(ms)]

4 Results

A computer simulation conducted using ANSYS Fluent software presented the thermal behavior of the air-fluid in two triangular cavities of 3D-printed walls. Four numerical simulations were performed, two considering the advective term, with a value of -9.81 m/s² on the Y axis, and two without the advective term. For the comparative analysis, a cross-sectional examination was conducted along the main direction of heat flow in both cavities. Figures 6 and 7 show the temperature distributions and velocity magnitudes resulting from these simulations.

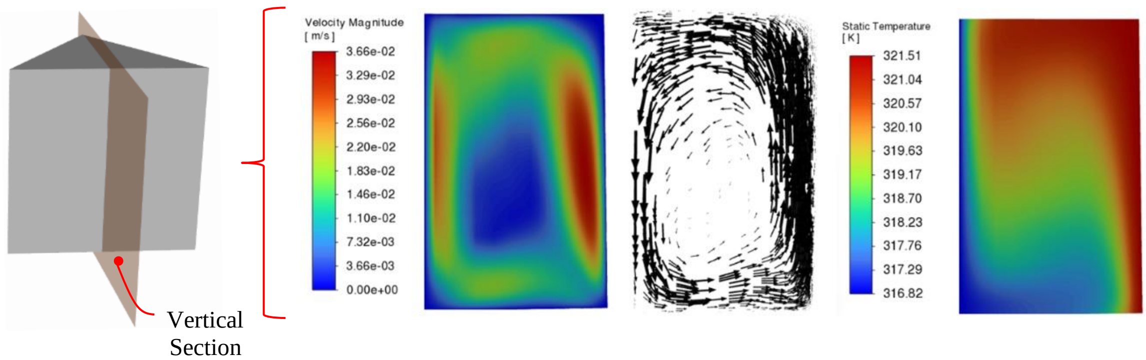

Figure 6. Distribution of velocity magnitudes (left) and velocity vectors (center) and static temperature distribution (right) in cavity 1 resulting from the simulations considering the advective term.

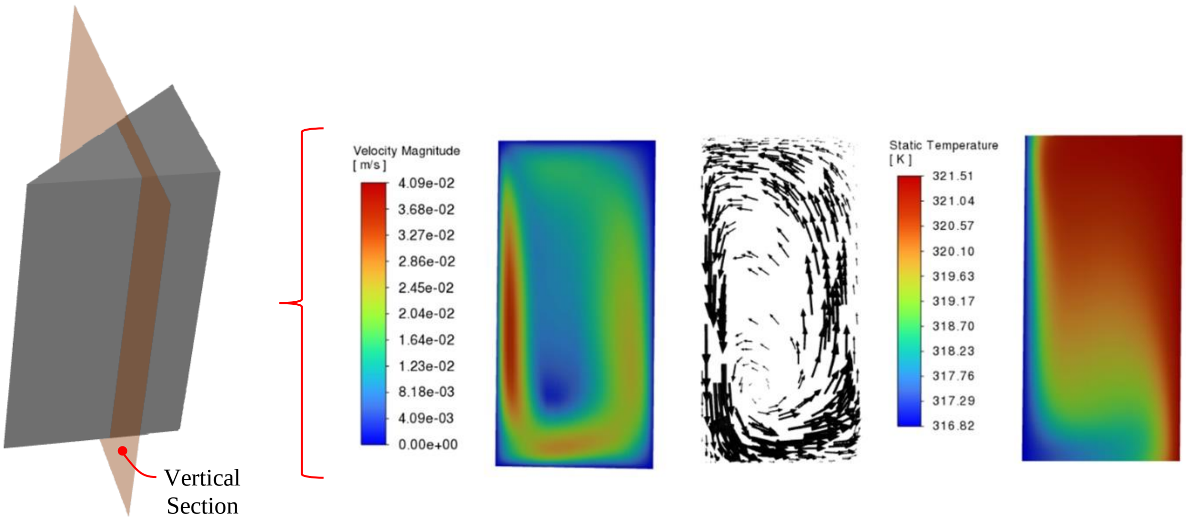

Figure 7. Distribution of velocity magnitudes (left) and velocity vectors (center) and static temperature distribution (right) in cavity 2 resulting from the simulations considering the advective term.

Figure 8 correspond to the simulations without the advective term, showing the temperature profile of the two air cavities.

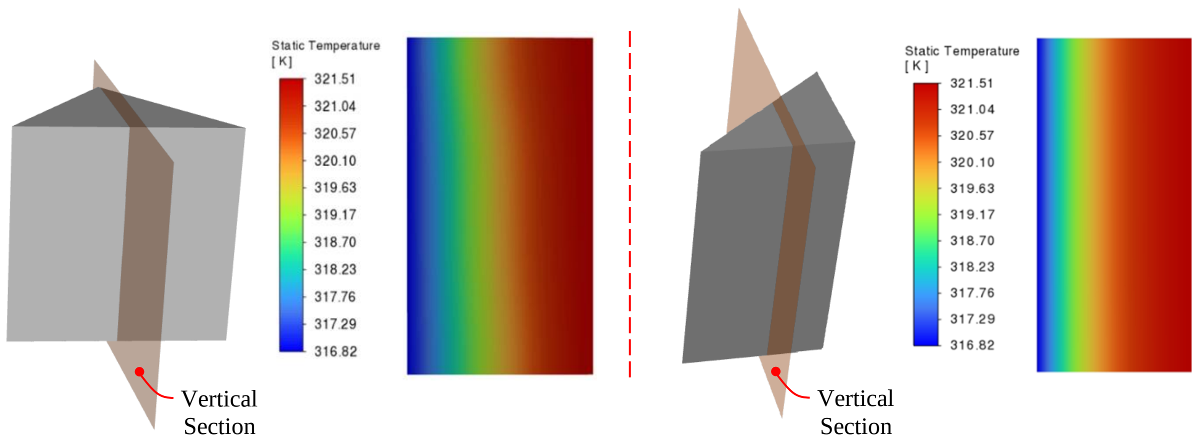

Figure 8. Static temperature distribution in cavity 1 (left) and cavity 2 (right) resulting from the simulations without the advective term.

It is noted that, by including gravity in the computer modeling, it is possible to identify the movement of the fluid that occurs in the air cavities. When comparing the results of the simulations with and without the advective term, it can be seen that the absence of this term transforms the problem into a problem of heat conduction, which does not represent real-world conditions. Gravity induces variations in fluid density, causing warm air to rise and cold air to descend, which drives convective motion. Therefore, without the advective term, the simulation does not capture the fluid dynamics, leading to results that do not adequately represent the complexity of the observed thermal phenomena.

To complete the analysis, a study of the total heat flow across the cavity surfaces was conducted, relating it to the temperature variation between each surface layer and its adjacent layers. This procedure allowed for the determination of the convective heat transfer coefficient (HTC) in different regions of the air cavities. The computational simulations revealed increased HTC values at the areas where surfaces intersect. In Cavity 1, the mean HTC values for surfaces T4, T5, and T7 were 19.8 W/m²K, 19.6 W/m²K, and 13.5 W/m²K, respectively. At the interface between surfaces, HTC reached 428.2 W/m²K at interfaces T4-T7 and T5-T7, while the T4-T5 interface had an HTC value of 202.2 W/m²K. In Cavity 2, the mean HTC values for surfaces T5, T6, and T7 were 16.7 W/m²K, 24.9 W/m²K, and 22.4 W/m²K, respectively. At the interfaces, the HTC values were 215.7 W/m²K at the T5-T6 interface, 330.1 W/m²K at the T6-T7 interface, and 440.3 W/m²K at the T7-T5 interface.

The average HTC values found are consistent with the standard HTC values reported in the literature for laminar airflow (10–25 W/m²K) in contact with concrete walls. These findings are consistent with those used in preliminary simulations of the experiment, considering only heat transfer through the wall (without accounting for the cavities) and using the air temperature measured within the cavities as a boundary condition, in accordance with Newton's law of cooling.

5 Discussion and conclusions

It is clear that advection plays a significant role in the heat transfer process in this scenario. Although a simplified 2D simulation can provide preliminary results, a three-dimensional approach is necessary for a more comprehensive analysis, allowing for a detailed assessment of the thermal behavior. This is because advective heat flow predominantly occurs in the vertical direction under the influence of gravity, which limits the effectiveness of a two-dimensional model in accurately representing the problem. Additionally, due to the triangular base shape, the central flow is always influenced by the walls. Therefore, a 3D simulation is more suitable for capturing the complex characteristics of the problem.

The simulation also reveals that the flow regime is laminar and has permanent characteristics. This way, a turbulence model is not required, significantly simplifying the model and reducing the cost of 3D simulation. In addition, with laminar flow, it is possible to use the symmetry of the problem to reduce the mesh by half, further reducing the computational cost of 3D simulation. In turbulent flows, the use of symmetry is not ideal, especially when using models such as LES (Large Eddy Simulation). In addition, since the problem has a steady regime, a transient analysis is not necessary.

With this information, it becomes simpler to model the full heat transfer simulation required to simulate the 3D-printed wall experiment using minimal computational resources and mathematical complexity. Therefore, the next step is to develop a 3D model that encompasses both fluid and solid, solving the problem of conjugate heat.

Acknowledgements. The authors are partially supported by the Brazilian funding agencies CNPq, and FAPERJ. This study was financed in part by the Coordenação de Aperfeiçoamento de Pessoal de Nível Superior — Brasil (CAPES) — Finance Code 001.

References

[1] T. Wangler et al., "*Digital Concrete: Opportunities and Challenges,*" RILEM Technical Letters, vol. 1, p. 67, Oct. 2016, doi: 10.21809/rilemtechlett.2016.16

[2] J, V.; SINGH, P. *Comparative analysis of concrete 3D printing and conventional construction technique for housing*. Em: Innovative Processes and Materials in Additive Manufacturing. [s.l.] Elsevier, 2023. p. 177–190.

[3] ANDRADE, R. V., "*Avaliação do Desempenho Térmico de Paredes de Concreto Construídas por Impressão 3D*". Dissertação de Mestrado, Universidade Federal do Rio de Janeiro, 2023.

[4] Opoku, F., Uddin, M., Atkinson, M., 2023. "*A review of computational methods for studying oscillating water columns – the Navier-Stokes based equation approach.*" Renew. Sustain. Energy Rev. (ISSN: 1364-0321) 174, 113124. http://dx.doi.org/10.1016/j.rser.2022.113124, URL https://www.sciencedirect.com/science/article/pii/S136403212201005X.